BM@N Note

K+/π+ for the interactions of the argon beam of the kinetic energy of 3.2 AGeV with C, Al, Cu, Sn targets.

BM@N configuration in the argon beam run

The argon beam run of the BM@N detector was performed in March 2018. The view of the BM@N setup used in the run is presented in Fig. 1 (left). The configuration of the central tracker was based on three planes of forward silicon detector and six GEM detectors with the size of 163x45 cm^2. (Fig. 1 (right)). The GEM tracking detectors were arranged above the beam to have the beam passing through the hollow at the bottom of the detector. Each successive GEM station was rotated by 180° around the vertical axis. It was done to have the opposite electron drift direction in the successive stations in order to avoid a systematic shift of reconstructed tracks due to the Lorentz angle in the magnetic field. The research program was devoted to measurements of inelastic reactions Ar+A → X with the beam kinetic energy of 3.2 AGeV and different targets: C, Al, Cu, Sn, Pb.

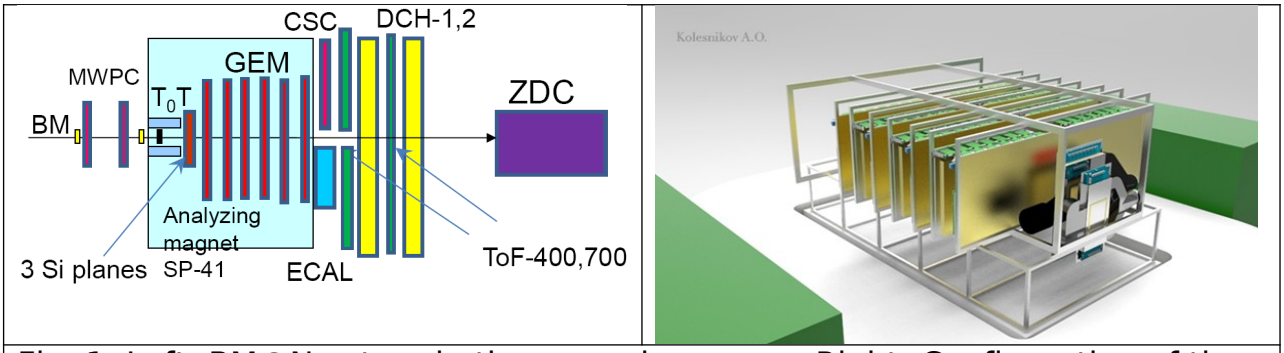

Fig. 1. Left: BM@N set-up in the argon beam run. Right: Configuration of the forward silicon and GEM detectors.

In the present analysis the experimental data from the GEM detectors, cathode strip chamber, ToF-400 mRPC detectors, trigger barrel and silicon multiplicity detectors, beam, veto and T0 counters were used. Scheme of identification is shown in Fig. 2.

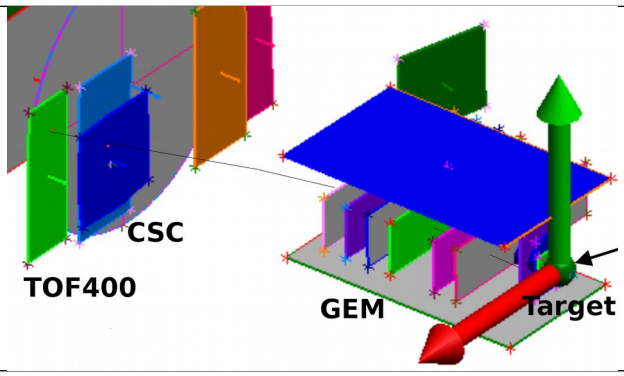

Fig. 2. Scheme of identification.

The event samples of Ar+A collisions were produced with the DCM-QGSM event generator. The passage of particles through the setup volume was simulated with the GEANT program integrated into the BmnRoot software framework. To properly describe the GEM detector response in the magnetic

field the microsimulation package Garfield++ was used. The dependencies of the Lorentz shifts and the charge distributions on the readout planes on the drift distance were parameterized and used in the GEM digitization part of the BmnRoot package. The details of the GEM simulation are given in the paper [DeuteronPaper]. The detector alignment procedure is described in the talk [Roufanov]. The track reconstruction method was based on a so-called “cellular automaton" approach [CBM1].

Event selection criteria:

1. Number of tracks in selected events: positive >=1, negative >=1; ???
2. Number of tracks in the primary vertex PV: >=1; ???
3. Beam halo, pile-up suppression within the readout time window: number of signals in the start detector: T0=1, number of signals in the beam counter: BC2=1, number of signals in the veto counter around the beam: Veto=0;
4. Pile-up suppression: total number of hits in GEM <440; ???
5. Trigger condition in the barrel multiplicity detector and forward silicon detector: number of signals BD>2 or BD>3 or Si>2 or Si>3 or (BD>1 and Si>2);

The event suppression factors (in %) of selection criteria 3-4 applied to eliminate beam halo and pile-up events in interactions of Ar+C, Ar+Al, Ar+Cu.

The total suppression factors from column 6 are applied to reduce the recorded beam fluxes and luminosities which are summarized in a table below.

Number of triggered events, beam fluxes and integrated luminosities collected in 3.2 AGeV argon beam.

Interactions, target thickness	Number of triggers / 10^6	Integrated beam flux / 10^7	Integrated luminosity / 10^{30} cm^{-2}
Ar+C (? mm)	?	?	?
Ar+Al (?mm)	?	?	?
Ar+Cu (?mm)	?	?	?
Ar+Sn (?mm)	?	?	?

K+ and π+ meson selection criteria:

- Number of GEM hits per track > 4
- Hit in CSC, residual of CSC hit to GEM track < 3 cm.
- Hit in ToF-400, residual of ToF-400 hit to GEM+CSC track in horizontal plane < 4 cm and in vertical plane < 4 cm
- Total momentum range of positive tracks: 0.5 < p_{pos} < 2 GeV
- Distance of track to the primary vertex in horizontal plane < 4 cm
- Distance of track to the primary vertex in vertical plane < 1.5 cm

On the Fig. 3 results of matching of CSC hits to GEM tracks and ToF-400 hits to GEM+CSC tracks are shown. Sigma for CSC hits to GEM tracks distribution about 8 mm. Sigma for ToF-400 hits to GEM+CSC tracks distribution about 6 mm.

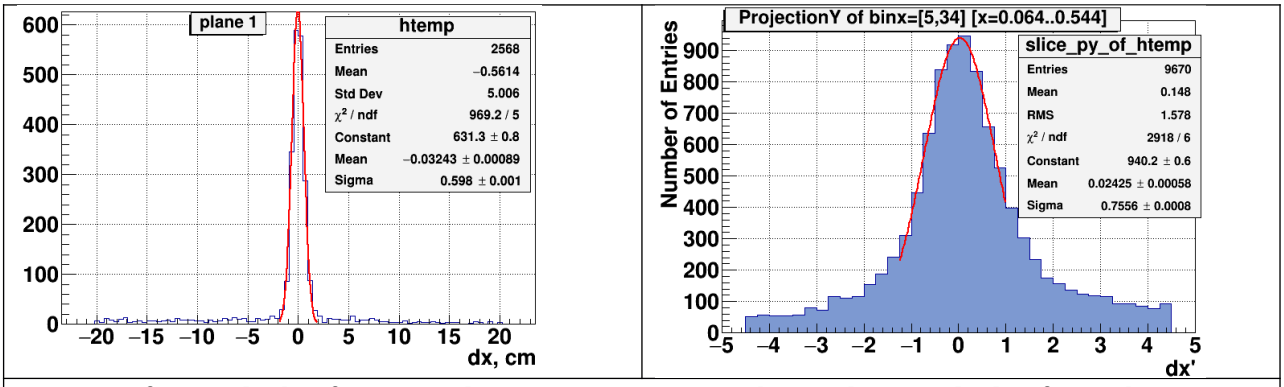

Fig. 3. Left: Residuals of ToF-400 hits to GEM+CSC tracks. Right: Residuals of CSC hits to GEM tracks.

Selection criteria which are shown above are common for all identified particles. Full set of identified particles is presented on the left side of the Fig. 4. Identification technique allows to identify positrons, pions, kaons, protons and some light nuclei (helium 3 and tritium). Deutrons and helium 4 are combined in the single band due to close mass to charge ratio. To separate them additional dE/dx information is needed.

As it shown on the right side of the Fig. 4 during the K+/π+ analysis process time resolution less than 90 ps measured by ToF-400 was achieved.

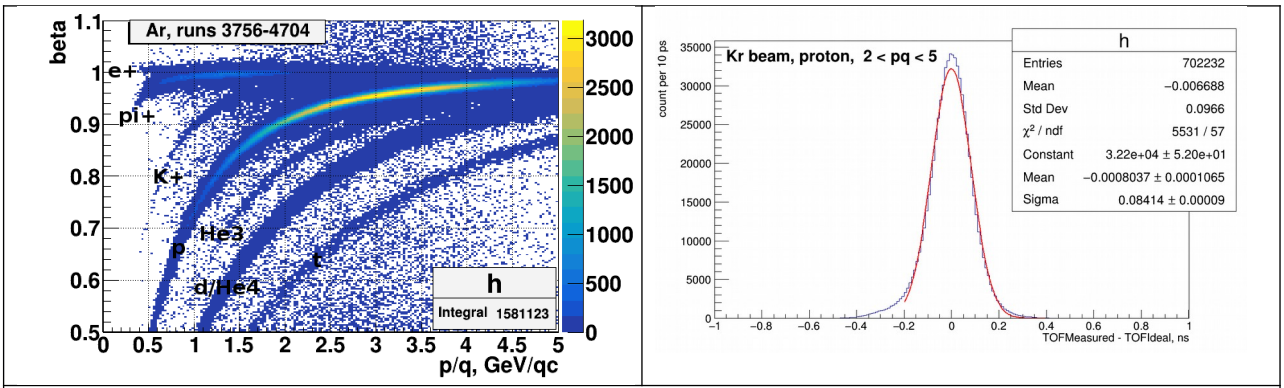

Fig. 4. Left:Distribution of the beta velocity as a function of the total momentum. Right: Time resolution of ToF-400.

Mass spectra of identified particles reconstructed in interactions of Ar+Al, Cu, Sn are shown in Fig. 5.

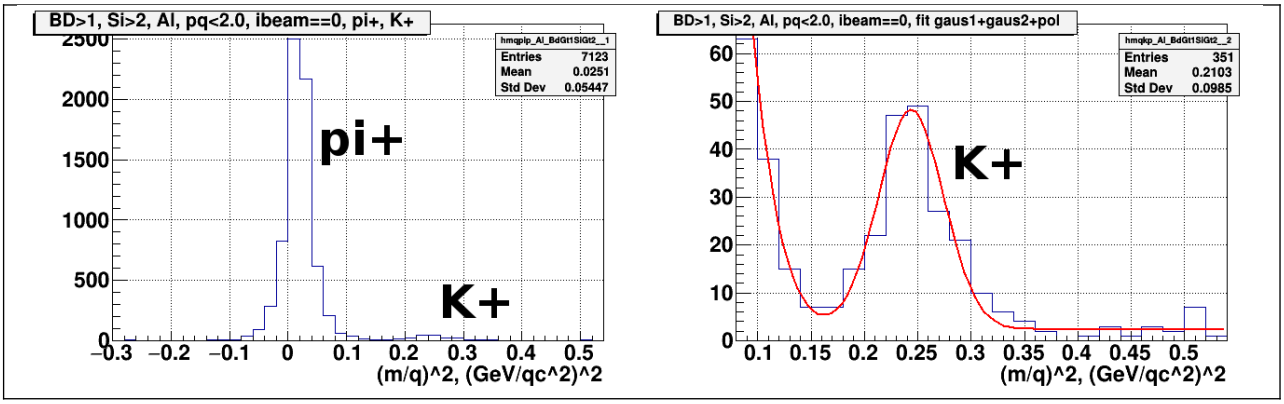

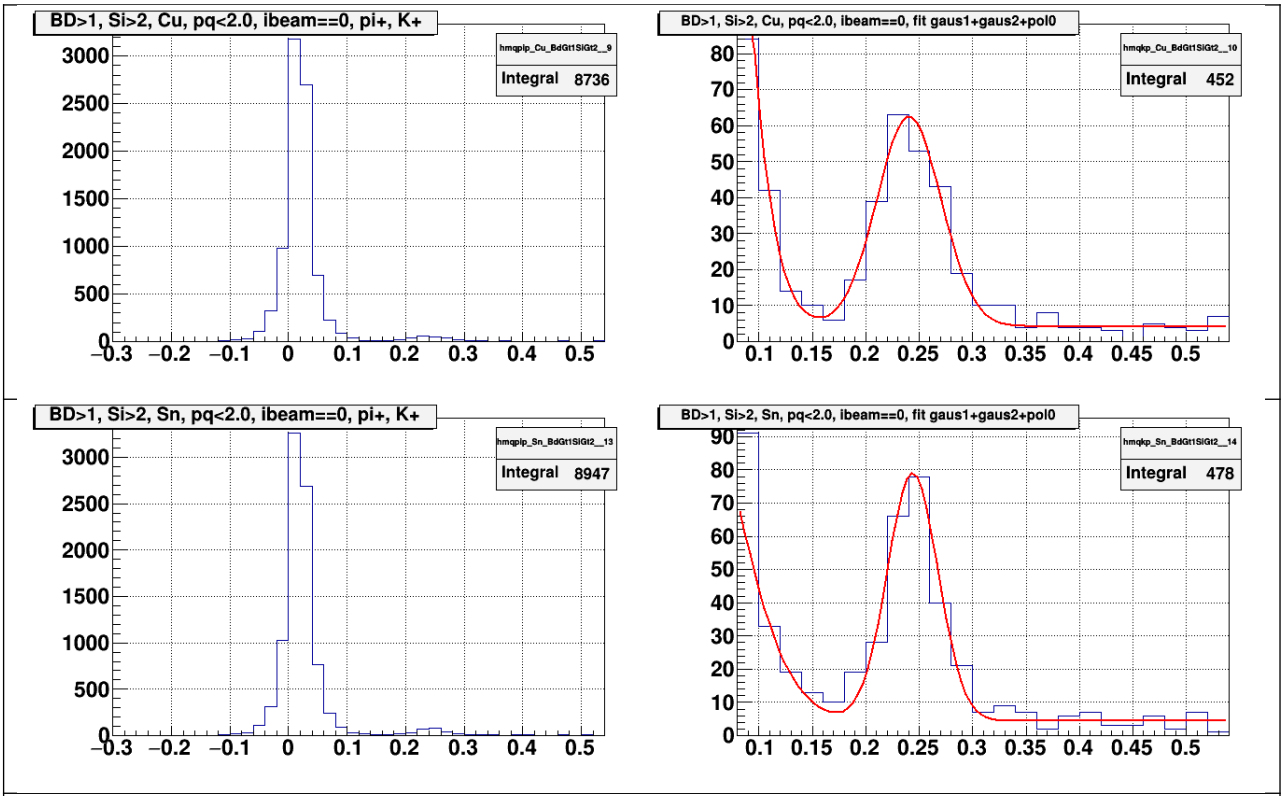

Fig. 5. Squared mass distributions of identified particles measured in interactions Ar+Al,Cu,Sn.

The K+ and π+ meson signals were parametrized by two Gaussians, the background of unidentified particles was fitted assuming a flat distribution. The numbers K+ and π+ mesons were calculated within ±3(???) sigma of the Gaussians. The K+ and π+ meson signals in intervals of the transverse momentum p_T and total momentum p were reconstructed using same fit procedure. The number of K+ and π+ mesons were calculated in the p_T and total momentum intervals within the same ±3 sigma (?) as for the full measured range. To estimate the systematic errors of the K+ and π+ meson signal extraction, the numbers of K+ and π+ mesons were also calculated assuming linear behavior of the unidentified particles. The difference in the K+ and π+ meson numbers was treated as a systematics error.

Table 1. The statistics of K+ and π+ mesons reconstructed in the kinematical range 0.5<p<2 GeV/c and 0.05<pT<0.4 GeV/c in Ar+C, Al, Cu, Sn interactions.

Trigger/Target	N_{K+}	$N_{\pi+}$
BD>1&&Si>2/C	31.4±8.7	1691.6±41.7
BD>3/C	31.3±8.3	1980.5±45.2
BD>1&&Si>2/Al	178.2±16.2	9626.1±98.8
BD>3/Al	214.0±16.5	10261.0±101.7
BD>1&&Si>2/Cu	222.7±17.3	8350.1±92.5
BD>3/Cu	121.1±13.6	5019.4±71.6

BD>1&&Si>2/Sn	235.3±18.3	8539.2±93.6
BD>3/Sn	144.6±14.0	4645.1±69.0

K+/π+ ratio, measured in data with trigger conditions BD>1,Si>2 and BD>3, plotted as a function of the target atomic number on the left side of the Fig. 6. K+/π+ ratio, averaged over data with trigger conditions BD>1,Si>2 and BD>3, plotted on the right side of the Fig. 6.

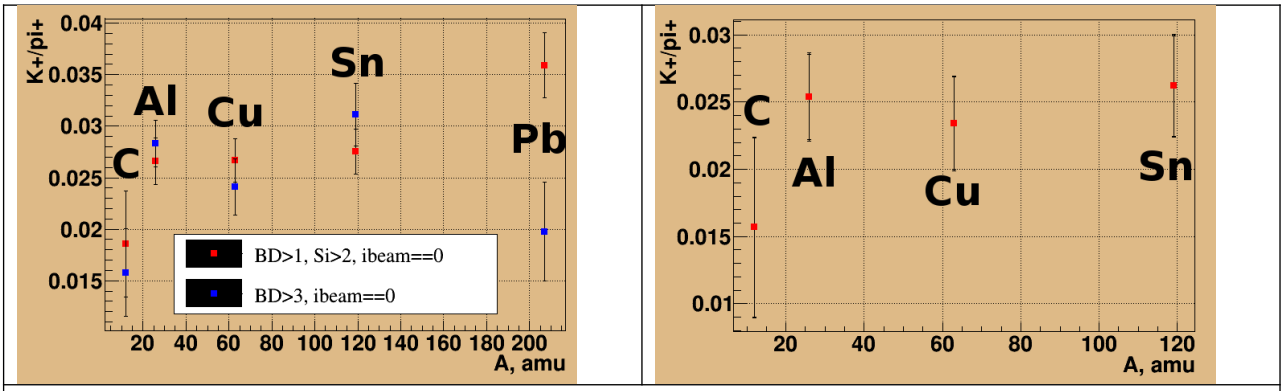

Fig. 6. Left: K+/π+ ratio, measured in data with trigger conditions BD>1,Si>2 and BD>3, plotted as a function of the target atomic number. Right: K+/π+ ratio, averaged over data with trigger conditions BD>1,Si>2 and BD>3.

To evaluate the K+ and π+ acceptance, detection and reconstruction efficiencies, minimum bias interactions of 3.2 AGeV argon beam with C, Al, Cu, Sn targets were generated with the DCM-QGSM generator. The generated particles traced through the BM@N geometry using the GEANT simulation and reconstructed using the BMNROOT analysis framework. Experimental and Monte Carlo distributions of number of hits per track are presented in Fig. 7.

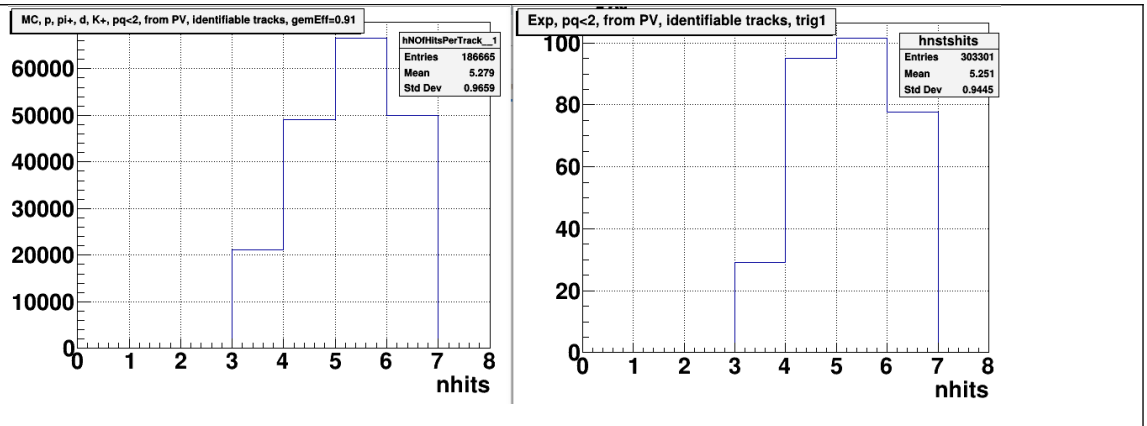

Fig. 7. Left: Monte Carlo distribution of number of hits per track. Right: Experimental distribution of number of hits per track.

Distributions of the total momentum and transverse momentum of K+ and π+ are presented in Figs. 8 and 9.

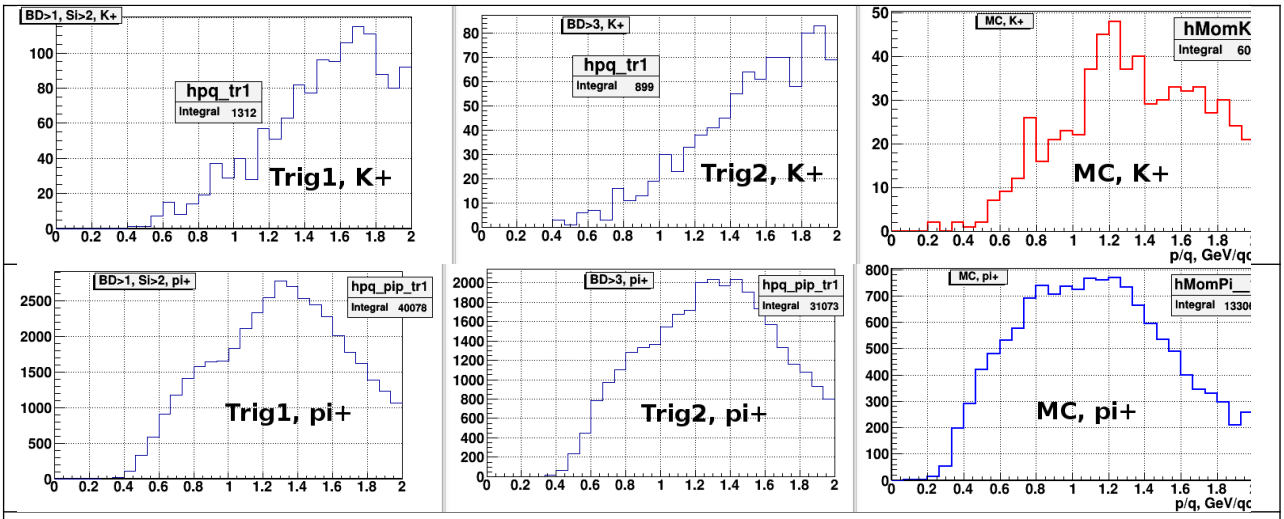

Fig. 8. Comparison of experimental total momentum distributions (left and middle plots) and Monte Carlo simulation of events generated with the DCM-QGSM model (right)

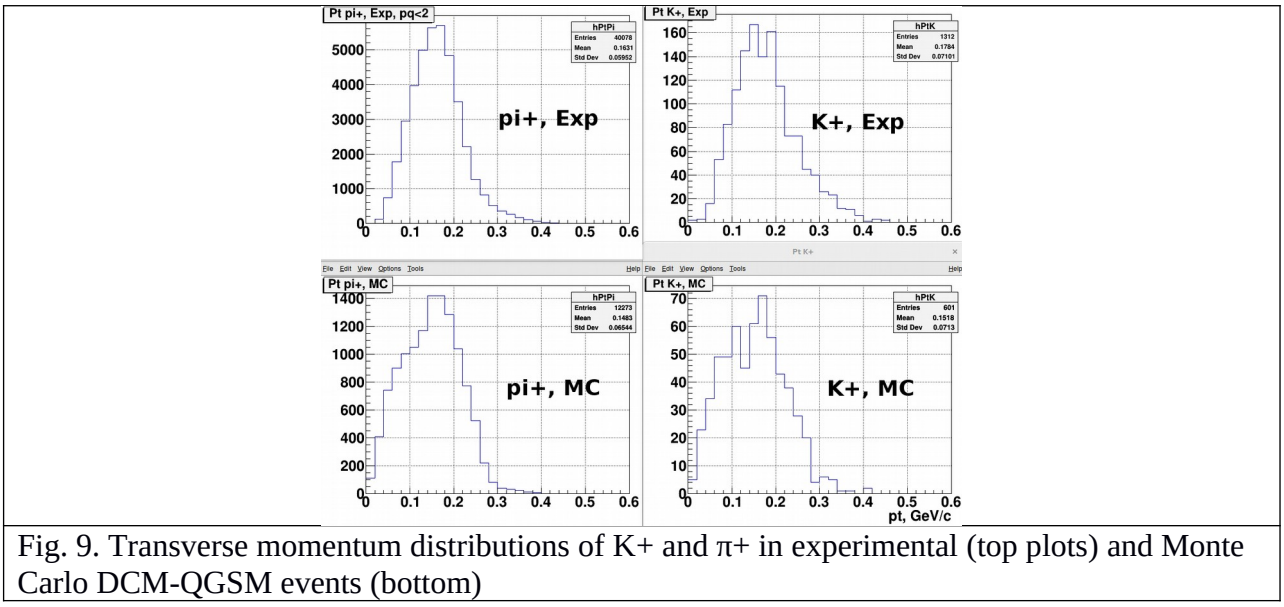

Fig. 9. Transverse momentum distributions of K+ and π+ in experimental (top plots) and Monte Carlo DCM-QGSM events (bottom)

To reproduce the detector effects in the efficiency the simulated products of Lambda hyperon decays (p,π-) were embedded into real experimental events of Ar+C, Ar+Al, Ar+Cu interactions. Simulated amplitude signals in the Forward Silicon and GEM detectors were added to the ADC stream of the recorded signals in the Forward Silicon and GEM detectors. The experimental distribution of GEM hit residuals to tracks is presented in Fig.7a. The corresponding distribution for embedded tracks of Lambda decay products are shown in Fig. 7b. The invariant mass spectrum of (p,π-) pairs reconstructed in the experimental events of Ar+Cu interactions with embedded Lambda hyperon decay products is illustrated in Fig.7. The Lambda signal is reproduced by a Gaussian parametrization with sigma ??? , which is consistent with the sigma of the experimental Lambda distribution.

The resulting Lambda reconstruction efficiency which is the ratio of the number of reconstructed Lambda hyperons to the number of generated ones in the intervals of (p_T,y) could be

decomposed into the following components: $\varepsilon_{rec} = \varepsilon_{acc} \cdot \varepsilon_{emb} \cdot \varepsilon_{cuts}$. The definition of every term is given in Table 2. The actual values of efficiencies (ε_{acc}, ε_{emb}, ε_{cuts}) calculated for Ar+Cu interactions in the y and p_T bins are shown in Fig.8. The combined reconstruction efficiencies ε_{rec} calculated for Ar+C, Ar+Al, Ar+Cu interactions are presented in Fig.9.

Table 2. Lambda hyperon reconstruction efficiency decomposition

Reconstruction efficiency	$\varepsilon_{rec} = \varepsilon_{acc} \cdot \varepsilon_{emb} \cdot \varepsilon_{cuts}$
Λ geometrical acceptance in GEM detectors	$\varepsilon_{acc} = N_{acc}(y,p_T) / N_{gen}(y,p_T)$
Efficiency of reconstructions embedded Λ	$\varepsilon_{emb} = N_{emb}(y,p_T) / N_{acc}(y,p_T)$
Efficiency of Λ selection: kinematical and special cuts	$\varepsilon_{cuts} = N_{cuts}(y,p_T) / N_{emb}(y,p_T)$

Correction to the trigger efficiency.

Table 2. K+/π+ correction to the trigger efficiency evaluated for events with identified K+ and π+ tracks in interactions of argon beam with C, Al, Cu, Sn targets.

Trigger	*BD>1 && Si>2*	*BD>3*
$C_{TrigEff}$	1.1347	1.0371

The systematics of the Lambda reconstruction efficiency was estimated by embedding the Lambda decay products into data samples with different trigger conditions (BD>=2 and BD>=3).

π+ can appear both in the events with high multiplicity and in the events with low multiplicity. K+ mainly appear in the events with high multiplicity. Triggers which were used in the experiment rejected more events with low multiplicity. We expect that triggers increasing K+/π+. To take into account trigger efficiency we calculated K+/π+ without and with each trigger. Then we got the ratio of these two K+/π+ for each trigger.

$C_{trigEff}$(Trig)=K+/π+(with Trig)/K+/π+(without Trig).

Values of $C_{trigEff}$ for two triggers are presented in the table 2.

The cross section σ_Λ and yield Y_Λ of Lambda hyperon production in Ar+C, Ar+Al, Ar+Cu interactions are calculated in bins of y and p_T are according to the formulas:

$\sigma_\Lambda(y,p_T)=N_{rec}^{\Lambda}(y,p_T) / (\varepsilon_{rec}(y,p_T)\cdot\varepsilon_{trig}\cdot L)$	$Y_\Lambda(y,p_T) = \sigma_\Lambda(y,p_T) / \sigma_{inel}$

Where L is luminosity, N_{rec}^{Λ} - number of reconstructed Lambda hyperons, ε_{rec} – combined efficiency of Lambda hyperon reconstruction defined in Table 2, ε_{trig} – trigger efficiency, σ_{inel} – cross section for minimum bias inelastic interactions. The cross section for inelastic Ar+C interactions is taken from the measurement [AngelovCC]. The cross sections for inelastic Ar+Al, Ar+Cu interactions are taken from the predictions of the DCM-QGSM model which are consistent with the results calculated by the formula: $\sigma_{inel} = \pi R_0^2 (A_P^{1/3} + A_T^{1/3})^2$, where R_0 = 1.2 fm is an effective nucleon radius, A_P and A_T are atomic numbers of the beam and target nucleus [HadesL0]. The uncertainties for Ar+Al, Ar+Cu inelastic cross sections are estimated by using

the alternative formula: $\sigma_{inel} = \pi R_0^2 (A_P^{1/3} + A_T^{1/3} - b)^2$ with $R_0 = 1.46$ fm and $b = 1.21$ [AngelovCC].

Interaction	Ar+C	Ar+Al	Ar+Cu
Inelastic cross section, mb	830±50	1260±50	1790±50

The yields of Lambda hyperons in minimum bias Ar+C, Ar+Al, Ar+Cu interactions are measured in the kinematical range on the Lambda transverse momentum of $0.1 < p_T < 1.0$ GeV/c and rapidity in the laboratory frame of $1.2 < y_{lab} < 2.1$. The rapidity of the beam-target nucleon - nucleon CM system calculated for an interaction of a 4 GeV/nucleon beam with a fixed target is $y_{CM} = 1.17$. The transformation of the y distribution to c.m.s.: $y^* = y_{lab} - y_{CM}$. The differential y spectra are measured in the transverse momentum range of $0.1 < p_T < 1.0$ GeV/c. They are presented in Fig 12. The predictions of the DCM-QGSM and URQMD models are shown for comparison. The differential p_T spectra are measured in the rapidity range of $1.2 < y_{lab} < 2.1$. In Fig.13 the measured p_T spectra are parametrized by the form: $1/p_T \cdot d^2N/dp_T dy = N \cdot \exp(-m_T/T)$, where $m_T = \sqrt{(m_\Lambda^2 + p_T^2)}$ is the transverse mass, the normalization N and temperature T are free parameters of the fit. The experimental spectra are compared with the predictions of the DCM-QGSM and URQMD models. The values of the temperature T, extracted from the fit of the p_T spectra, are summarized in Table 4.

reaction	Ar+C,Al, Cu,Sn
K+ Temperature, MeV	100±20±20 ?
π+ Temperature, MeV	

The systematic error of the K+/π+ is calculated via a quadratic sum of uncertainties rising from the following sources:

- Systematic errors of the momentum scaling (p → 0.96p)
- Systematic errors of ToF-400 strips correction to the proton band
- Systematics errors of ToF-400 strips dt-amplitude dependence fit
- Systematics errors of unidentified background fit

Values of relative systematic errors from the different sources are presented in the table 3.

Table 3. Relative systematic errors from the different sources.

Source of systematic error	Without 096pq scaling	Strips corrected to protons in 2<pq<5	dt vs amplitude alignment fit	Unidentified background fit
Value, %	2.8	0.3	0.2	1.9

Do we need to show pictures to illustrate each systematic error here?

Amount relative systematic error is about 3%. It is much lower than relative statistic error which is more than 12%.

We took into accout **correcion for acceptance and K+ and π+ decays**. For that purpose Monte Carlo simulation have been used. Total momentum spectra for generated and identifiable K+ and π+ are shown in Fig. 10. Under identifiable track we mean the track from the primary vertex with at least 5 GEM hits and ToF-400 hit.

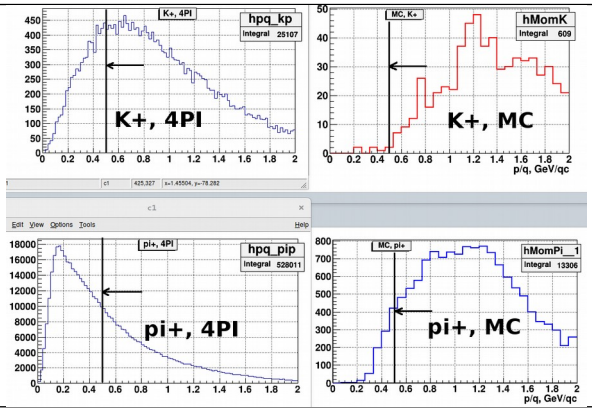

Fig. 10. Total momentum distributions of K+ (top row) and π+ (bottom row) in Monte Carlo DCM-QGSM events for generated (left column) and identifiable tracks (right column).

K+/π+(A) dependence with correction for trigger efficiency and correction for acceptance and decays is shown in Fig. 11. For all targets we applied the same correction for trigger efficiency and the same correction for acceptance.

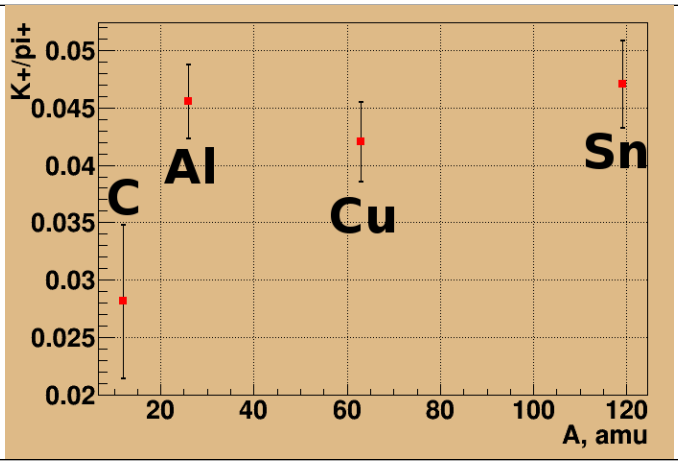

Fig. 11. K+/π+ ratio for C, Al, Cu and Sn targets, averaged over data with trigger conditions BD>1,Si>2 and BD>3, and corrected to the trigger efficiency and to the acceptance and decays.

To build **K+/π+(p)** dependence data for C, Al, Cu and Sn targets was combined. We have splitted identifiable total momentum range into 4 bins in such a way to have similar number of K+ in each bin. In each bin correction for trigger efficiency and correction for acceptance and decays have been calculated separately. K+/π+(p) is shown in Fig. 12.

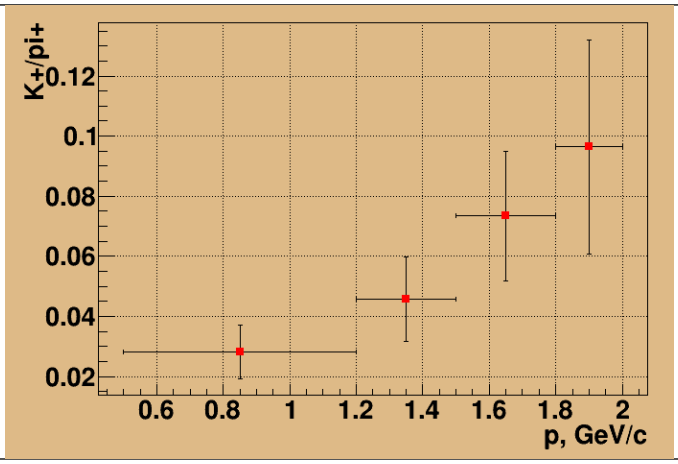

Fig. 12. K+/π+(p) dependence, averaged over data with trigger conditions BD>1,Si>2 and BD>3, and corrected to the trigger efficiency and to the acceptance and decays.

Data for **K+/π+(pt)** dependence for 4 targets was combined in the similar manner as for K+/π+ (p) dependence. Then transverse momentum range was splitted into 4 bins with similar number of K+ in each bin. In each bin correction for trigger efficiency and correction for acceptance and decays have been calculated separately. K+/π+(pt) is shown in Fig. 13.

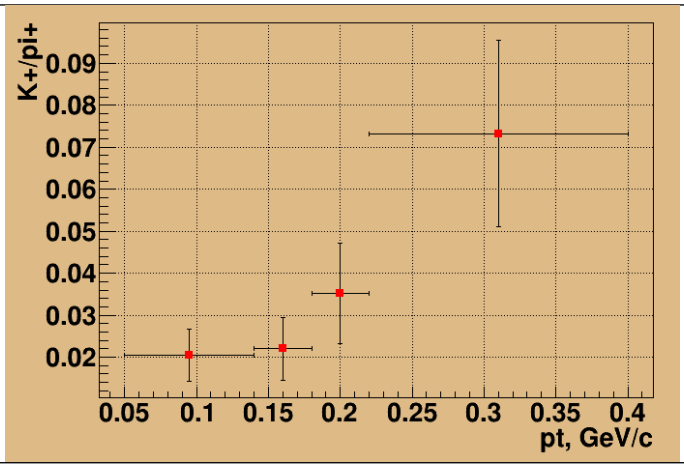

Fig. 13. K+/π+(pt) dependence, averaged over data with trigger conditions BD>1,Si>2 and BD>3, and corrected to the trigger efficiency and to the acceptance and decays.

Rapidity spectra for π+ and K+ are presented in the Fig. 14.

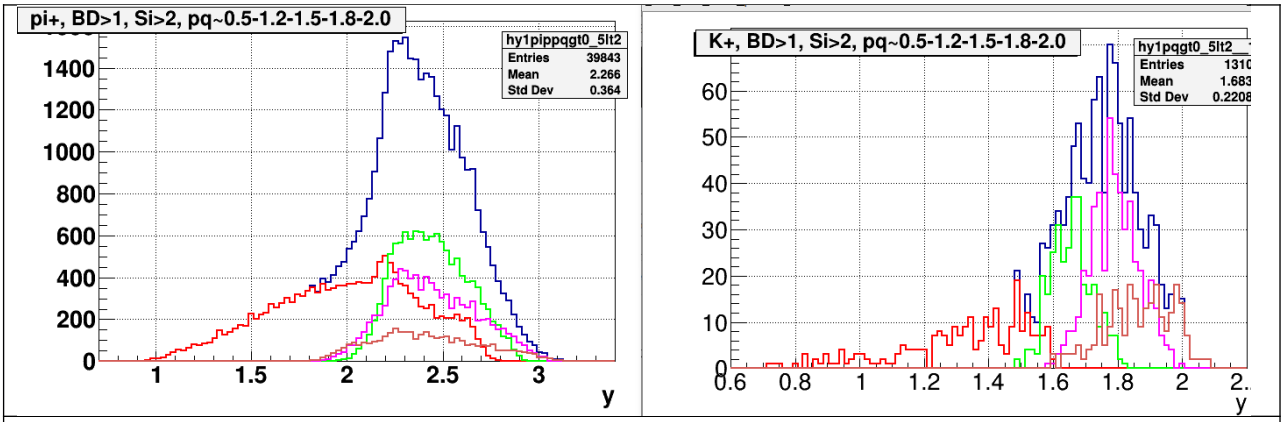

Fig. 14. Distributions of π+ on rapidity (y). Right: distributions of K+ on rapidity (y). Different curves represent different intervals in total momentum.

More details of K+/π+ analysis can be found in [K+/π+ analysis note in russian].

The integrated yields of Lambda hyperons produced in Ar+C, Ar+Al, Ar+Cu in minimum bias interactions in the kinematical range of 0.1 $<p_T<$ 1.0 GeV/c and 1.2 $<y_{lab}<$ 2.1 are summarized in Table 5. To extrapolate the measured yields to the full kinematical range the predictions of the DCM-QGSM and URGMD models are used. The model extrapolation factors and the estimated yields and cross sections of the Lambda hyperon production in Ar+C, Ar+Al, Ar+Cu minimum bias interactions are given in Table 5.

Table 5

Interaction	Ar+C	Ar+Al	Ar+Cu	Ar+Sn
Measured yields of K+ and π+ in $p_T<0.5$ GeV/c, 0.5<p<2 geV/c	±	±	±	
Extrapolation factors for K+ and π+ to the full kinematical range, DCM-QGSM				
Extrapolation factors for K+ and π+ to the full kinematical range, URQMD				
Yields of K+ and π+ in the full kinematical range	±	±	±	
Ratios of K+ and π+ in the full kinematical range	±	±	±	

The Lambda yields and production cross section in Ar+C interactions could be compared with the previous results of 23.2±2.5 mb [ArmutCC] and 24 ± 6 mb [ArakelianCC] measured in interactions of the carbon beam with the momentum of 4.2 GeV/c per nucleon (beam kinetic energy of 3.36 GeV per nucleon) with the propane chamber.

Interacting nucleus / reference	Beam momentum, kinetic energy	K+ / π+ yields	K+/π+,
C+C, HADES	2 AGeV	5.9±1.1±1.2	
Ar+KCl, HADES	1.76 AGeV		$2.8 \cdot 10^{-2}$ / 3.9
Ni+Ni, KaoS	1.91 AGeV		$7.59 \pm 0.49 \cdot 10^{-3}$
		K+: 0.0053±0.0005 π+: 0.79±0.09	$6.7 \cdot 10^{-3}$

To do list

1. K+ and π+ extrapolation factors from pT<0.5 GeV/c, 0.5<p<2 GeV/c to the full kinematical range using DCM-QGSM and URQMD models (Ar+C,Al,Cu,Sn)
2. K+ and π+ reconstruction efficiency in the range of pT<0.5 GeV/c, 0.5<p<2 GeV/c as a function of pT , total momentum and rapidity y.
3. Transformation from Lab to CMS in total momentum;
4. pT and total momentum spectra of K+ and π+ corrected to the reconstruction efficiencies

5. Ratio of yields of K+ and π+ in the full kinematical range
6. Systematic errors estimated by reweighting the Monte Carlo pt and total momentum distributions to adjust it to the measured momentum distributions

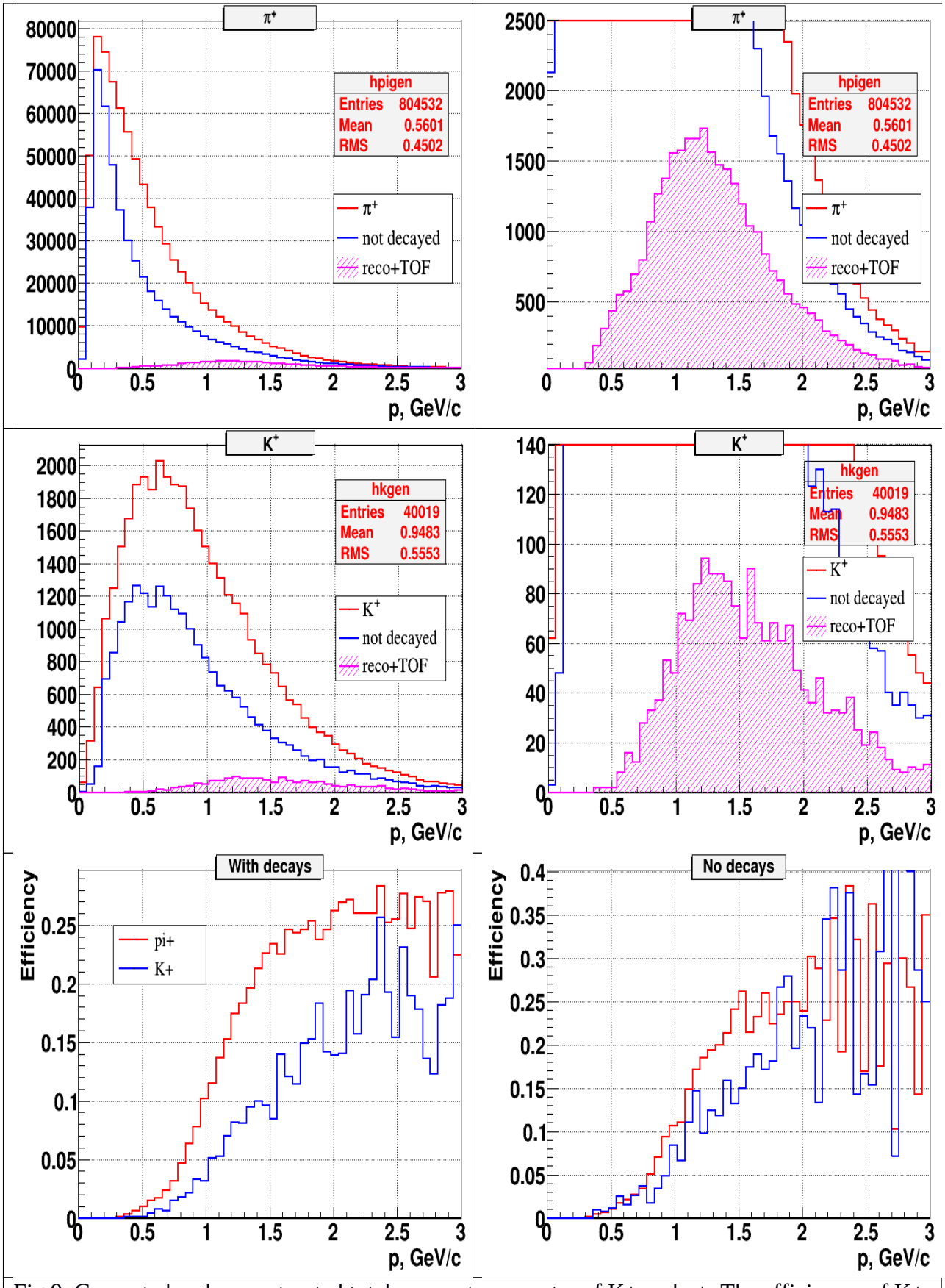

Fig.9. Generated and reconstructed total momentum spectra of K+ and π+. The efficiency of K+

and π+ reconstruction in dependence on the total momentum. The effect of different decay times is shown.

Fig.10.	

Fig. 11.	

Fig. 12.	

Fig. 13.	

Bibliography

[DeuteronPaper]
[Roufanov]
[CBM1]
[K+/π+ analysis note in russian]